

# Solving the structure of reaction intermediates by time-resolved synchrotron x-ray absorption spectroscopy

Qi Wang,<sup>1</sup> Jonathan C. Hanson,<sup>2</sup> and Anatoly I. Frenkel<sup>1,a)</sup>

<sup>1</sup>Physics Department, Yeshiva University, New York, New York 10016, USA

<sup>2</sup>Chemistry Department, Brookhaven National Laboratory, Upton, New York 11973, USA

(Received 29 August 2008; accepted 12 November 2008; published online 15 December 2008)

We present a robust data analysis method of time-resolved x-ray absorption spectroscopy experiments suitable for chemical speciation and structure determination of reaction intermediates. Chemical speciation is done by principal component analysis (PCA) of the time-resolved x-ray absorption near-edge structure data. Structural analysis of intermediate phases is done by theoretical modeling of their extended x-ray absorption fine-structure data isolated by PCA. The method is demonstrated using reduction and reoxidation of Cu-doped ceria catalysts where we detected reaction intermediates and measured fine details of the reaction kinetics. This approach can be directly adapted to many time-resolved x-ray spectroscopy experiments where new rapid throughput data collection and analysis methods are needed. © 2008 American Institute of Physics.

[DOI: [10.1063/1.3040271](https://doi.org/10.1063/1.3040271)]

## I. INTRODUCTION

*In situ* time-resolved (TR) spectroscopy and crystallography techniques are among the most common structural methods available to date for probing intermediate states during real time transformations in a large variety of systems of interest in physics, chemistry, structural biology, and materials science. For example, both TR x-ray diffraction (XRD) and x-ray absorption fine-structure (XAFS) spectroscopy have been recently applied to monitor the reduction and reoxidation behavior of pure or doped metal oxides [CuO,<sup>1</sup> Cu-ceria,<sup>2</sup> Au-ceria,<sup>3</sup> and Cu–MoO<sub>2</sub> (Ref. 4)] in water-gas-shift reactions. Another area of application of TR methods is the study of enzyme-catalyzed biological processes, which are characterized by perfect turnover and unique reaction pathways.<sup>5</sup> Vibrational spectroscopies,<sup>6</sup> magnetic circular dichroism,<sup>7</sup> and UV-visible and fluorescence spectroscopies<sup>8</sup> are more commonly applied in this field, due to their excellent sensitivity to protein structures, although TR-XRD (Refs. 9 and 10) and TR-XAFS (Refs. 11 and 12) have been also applied to study intermediate state structure and determine reaction kinetic constants of biological reactions. *In situ* TR-XAS (x-ray absorption spectroscopy) of most reactions involving enzymes is often done by the freeze-quench method,<sup>13</sup> which enables access to more rapid reaction rates (milliseconds to seconds) compared to the capabilities of the alternative cam-driven (quick extended XAFS or QEXAFS) mode (subseconds to seconds).

Despite their popularity for intermediate state detection, vibrational spectroscopies use a feature identification (“fingerprinting”) approach and thus are more suited for qualitative interpretation, though quantitative analysis can be done in some cases albeit indirectly.<sup>14,15</sup> In contrast, crystallographic techniques are superior in quantitative and direct de-

termination of the sample structure. However, the applications of these techniques are limited to ordered phases and, often, low temperatures when applied to biological samples. These techniques would be therefore useless when reaction intermediates are dilute, strongly disordered, or dispersed.<sup>12</sup> However, these are the most common conditions that occur in chemical or enzymatic catalysis as well as in environmental chemistry. It is in these rapidly emerging areas of science where both the use of XAFS and the development of new quantitative methods of intermediate state determination by XAFS are presently most sought. XAFS is sensitive to the local structure only, within the distance range of ~8 Å from the resonant (x-ray absorbing) atom and thus does not require a crystallized sample. In addition, it is element specific and can be used at low concentrations.<sup>12</sup> It can also be applied *in situ* under realistic reaction conditions (e.g., the gas atmosphere and pressure or sample temperature) in real time. Thus, TR-XAFS contains relevant information about real time phase composition and structure in the course of reaction, which cannot be uncovered by static techniques.<sup>16</sup>

One of the methods allowing detection of intermediates that many spectroscopic techniques offer is based on the examination of isosbestic points. This method relies on the presence or absence of the points where all spectra taken at different stages of the reaction intersect each other.<sup>17</sup> The presence of one or more isosbestic points is a sign of a direct transformation of reactants to products while the absence of isosbestic points indicates the formation of intermediate phase(s). However, this method can only indicate that the intermediates are present but not obtain their structure quantitatively. Principal component analysis (PCA) is a robust quantitative method of linear algebra, which allows the determination of the number of linearly independent components in the series of experimental spectra without making any model-dependent assumptions of their chemical nature

<sup>a)</sup>Author to whom correspondence should be addressed. Electronic mail: [anatoly.frenkel@yu.edu](mailto:anatoly.frenkel@yu.edu).

or structure. Two principal components indicate that reaction occurs without an intermediate, while three or more indicate that there are one or more intermediates. While first successful applications of PCA to phase speciation were reported for gas chromatography, mass spectrometry, and nuclear magnetic resonance data,<sup>18</sup> more recent reports demonstrate the power of combination of PCA and XAS.<sup>19–22</sup> Additionally, it was shown to be possible to advance this method further by actually identifying the intermediate phases and measuring their TR mixing fractions by fitting the abstract principal components obtained by PCA to various standard compounds [CuO–Cu<sub>2</sub>O–Cu for the CO reduction of CuO (Ref. 1) and MoO<sub>3</sub>–Mo<sub>18</sub>O<sub>52</sub>–MoO<sub>2</sub> for three phases in MoO<sub>3</sub> reduction in propene and MoO<sub>2</sub> oxidation in oxygen<sup>16</sup>]. The need for a more robust data analysis method, for standardless reaction phases, is especially timely due to the increasing use of advanced synchrotron facilities such as QEXAFS, dispersive XAFS, as well as methods of ultrafast x-ray spectroscopy, e.g., pump-probe methods.<sup>23</sup>

This paper presents a new analysis method based on combination of the PCA application to *in situ* TR-XAFS data coupled with theoretical modeling of the intermediate phase or phases. The method presented here can be summarized as follows: First, the number of intermediate phases is obtained model independently by PCA of *in situ* x-ray absorption near-edge structure (XANES) data. Second, the spectra of intermediate phase(s) are isolated from the experimental data for subsequent analysis. Third, theoretical modeling is performed on the EXAFS data corresponding to the intermediate phase and its local structure is determined. The power of this method is illustrated by examples of reduction/oxidation of copper/ceria system studied by QEXAFS.

## II. DETECTION, ISOLATION, AND THEORETICAL MODELING OF REACTION INTERMEDIATES USING PCA AND FEFF MODELING

As reaction progresses, changes in the XANES and/or EXAFS spectra reflect the changes in the absorbing atom's electronic and atomic structures during the reaction. One-step transformations, without an intermediate, would result in a two-component system

$$\chi(E, t) = x(t)\chi_R(E) + (1 - x(t))\chi_P(E), \quad (1)$$

where  $\chi(E, t)$  is the time-dependent XANES or EXAFS spectrum,  $\chi_R(E)$  and  $\chi_P(E)$  are the reactant and product spectra, and  $x(t)$  is the time-dependent mixing fraction. The number of principal components larger than two implies, in most cases, the presence of intermediates. In the former case (no intermediates), PCA may not be necessary since the presence of isosbestic points in EXAFS range manifests the one-step mechanism<sup>24</sup> and  $x(t)$  can be then obtained by a simple linear combination fit. For two-step reactions with one intermediate (the methods below can be easily extended to multistep reactions),  $\chi(E, t)$  can be presented as

$$\chi(E, t) = x(t)\chi_R(E) + y(t)\chi_I(E) + z(t)\chi_P(E), \quad (2)$$

$$x(t) + y(t) + z(t) = 1.$$

One of the main roles of TR spectroscopy experiments is to isolate the time  $t^*$  when  $y(t^*)=1$  and identify the structure of the intermediate phase. A notable exception when this may not be possible is a case when reaction branches out into several simultaneous processes (i.e., one or more intermediate phases coexist with reactants and/or products at all times). However, even in that case, PCA can be used to find out the number of phases.

In our approach, the first task (finding  $t^*$ ) is performed with PCA. The details of the method have been described previously.<sup>19,22</sup> In brief, the number of principal components is obtained, using XANES range of the TR spectra, to speed up this stage of the analysis.<sup>22</sup> In the case of spectroscopically silent elements (e.g., Zn),<sup>12</sup> EXAFS range can be used for this purpose as well.<sup>21,25</sup> Assume, for simplicity, that our analysis results in three principal components, suggesting one intermediate phase. One possibility would be to isolate the intermediate phase spectrum by fitting three components to a series of standard compounds that give the best fit, as suggested in previous works.<sup>1,16</sup> One of the standards would simulate the structure of the intermediate. This approach works only for relatively long-living intermediates with high to moderate crystalline order and structures that are similar to their bulk counterparts. The focus of this research, however, is on the analysis of those short-living, strongly dispersed and strongly disordered intermediates that appear in real reactions. The structures of such intermediates may differ strongly from those of relevant known compounds and, often, cannot be reliably refined by XRD. Moreover, the approach using linear fit to standard compounds is model dependent. In this method, we fit all spectra with two principal components instead and analyze the residuals. As expected, the residuals in the time intervals corresponding to the beginning ( $x=1$ ) and the end ( $z=1$ ) of the reaction are larger since each component has a spectral content corresponding to the reactants, products, and intermediate(s), not just the reactants and the products. An intermediate phase ( $y=1$ ) is isolated model independently from the rest of the species if the time interval is found:  $t^* - \Delta t/2 < t < t^* + \Delta t/2$  during which the residual is maximized as well.

Once the characteristic time  $t^*$  of the intermediate phase is identified, its EXAFS data  $\chi(t^*)$  can be analyzed conventionally by nonlinear least square fitting of theoretical EXAFS signal. The best fit result will provide the structural information (e.g., coordination numbers, bond lengths, and their disorders) that can be used in many cases to reliably identify the local structure of unknown samples. Section III presents an example of this analysis scheme described above.

## III. EXAMPLE: INTERMEDIATE PHASE ANALYSIS OF Cu-DOPED CERIA CATALYSTS

We illustrate this method of solving reaction intermediate structure problem by using an example of Cu *K*-edge QEXAFS spectra measured during rapid reduction and subsequent reoxidation of 20% Cu-doped Ceria (Ce<sub>0.8</sub>Cu<sub>0.2</sub>O<sub>2</sub>)

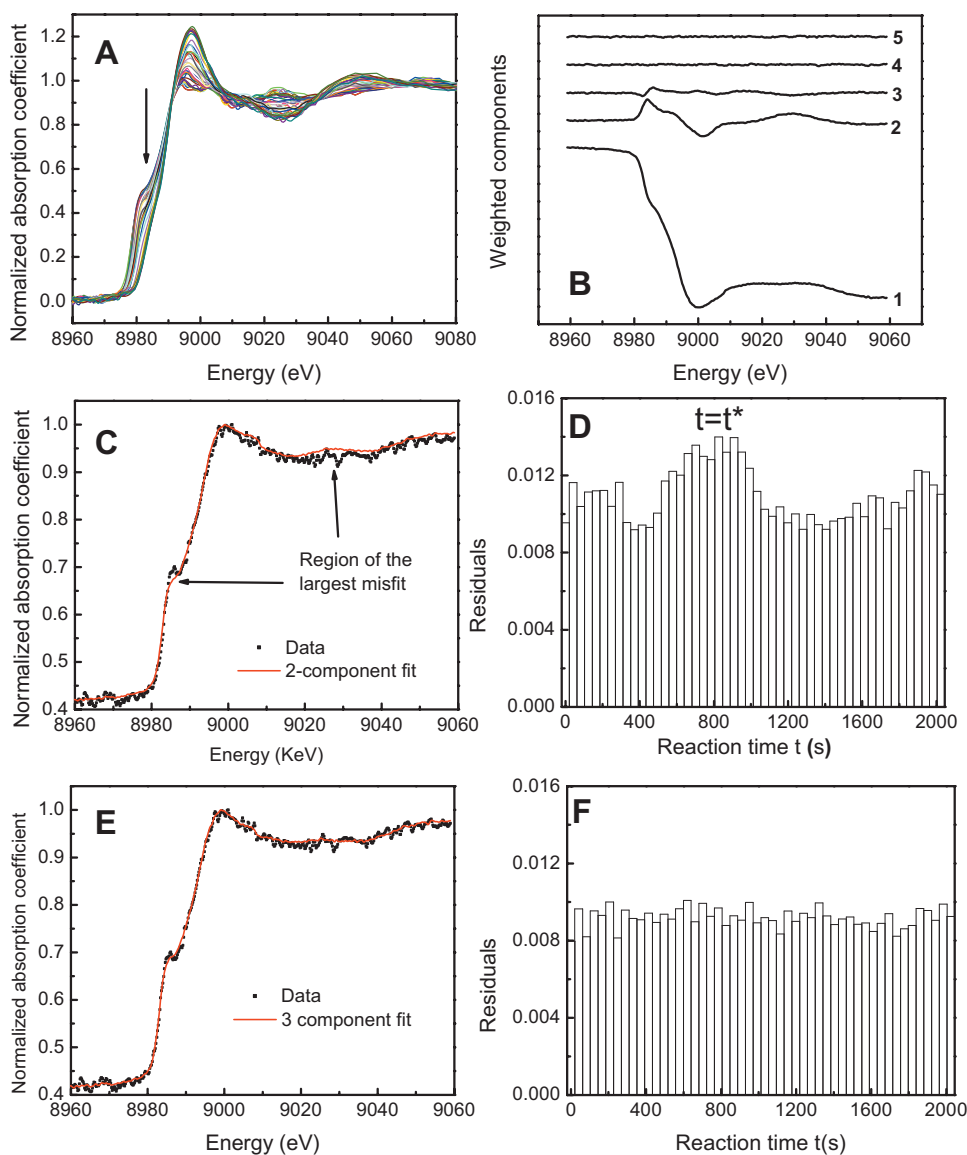


FIG. 1. (Color) PCA illustrating the method of trapping a reaction intermediate: (a) TR XANES of  $\text{H}_2$  reduction of  $\text{Ce}_{0.8}\text{Cu}_{0.2}\text{O}_2$  showing the structural evolution during the reaction (the arrow indicates reaction direction); (b) the first five components from PCA calculation weighted by eigenvalues; (c) representative spectrum (in dots) superimposed with the linear combination of two components (solid line); the arrows point to the largest misfits; (d) residual plots resulted from a two-component fit [the arrow points to the time stamp ( $t^*$ ) of intermediate]; (e) representative spectrum (dots) superimposed with the linear combination of three components (solid); (f) residual plot resulted from a three-component fit.

system. Experiments were performed at Beamline X18B of the National Synchrotron Light Source at Brookhaven National Laboratory using a QEXAFS monochromator and a custom-made data acquisition software.<sup>26</sup> The reduction and reoxidation cycles were carried out isothermally by using 5%  $\text{H}_2/\text{He}$  and 10%  $\text{O}_2/\text{He}$ , respectively. The cycles were run at two different temperatures: 200 and 300 °C. During each process of reduction or oxidation, up to 17 full XAFS scans, from 150 below to 1000 eV above the Cu  $K$ -edge (8979 eV), were recorded in 30 s time interval. Thus, the best time resolution achievable with these parameters is  $\sim 2$  s/scan.

Raw data were processed by a custom-made software.<sup>27</sup> Since no changes have been observed to occur during the short 30 s acquisition time intervals, all 17 spectra in each 30 s interval were merged to be used as one time point in the subsequent data analysis process. Thus, the effective time resolution in this example was 30 s. In addition, for theoretical modeling, steady phase spectra were averaged over twenty 30 s intervals for the reactant and the product to reduce random noise.

Figure 1(a) displays a group of spectra in the XANES

region for the  $\text{H}_2$  reduction of  $\text{Ce}_{0.8}\text{Cu}_{0.2}\text{O}_2$  at 200 °C. The reduction progress is manifested by the intensity decrease in the copper main absorption peak intensity with reaction time. As shown, no isosbestic points can be found in the series of TR XANES spectra for the reaction, ruling out a one-step reaction. To obtain the number of intermediate phases PCA was used in this case.

In this work, we used the “PCA” data analysis package developed by Wasserman and co-workers<sup>1,22,28</sup> available for solving problems of TR-XAFS data analysis. To determine the number of distinct phases in this process, we used XANES spectra  $\mu(E)$  in the energy range of 8959–9059 eV. The first five eigenvectors, or abstract components (sorted in the descending order of their respective eigenvalues), from the PCA calculation, are displayed in Fig. 1(b). This figure demonstrates that while the first two components clearly dominate the spectra in the edge region where the changes between  $\text{Cu}^{2+}$ ,  $\text{Cu}^+$ , and Cu are the greatest, the third component appears to be above noise in this region. However, in this case where noise in data may be substantial, we did not rely on the visual observation or the “screep test,” which is

often used in PCA. Instead, we calculated the best approximation of the data by a different number of principal components and examined residuals.

When the spectra were fitted with a linear combination of the two principal components [Fig. 1(c)], the biggest misfit was observed in the region 8980–8983 eV (where the change between  $\text{Cu}^{2+}$  and  $\text{Cu}^+$  is the greatest). This observation indicates the presence of one or more intermediate phases, in agreement with previous tests, including the absence of isobestic points in the data. Fit residuals shown in Fig. 1(d) have a distinct maximum between  $t=660$  and 990 s measured from the beginning of the reaction.

As expected, the fit quality is greatly improved when we used three principal components to reproduce the spectra. Figure 1(e) illustrates that the fit in the 8980–8983 eV range has improved drastically. Figure 1(f) demonstrates that the residuals do not vary outside the statistical noise level throughout the entire duration of the reaction. Together, these observations support our conclusion that three principal components reproduce the data reliably throughout the entire XANES energy range at all times, indicating that exactly three distinct phases of Cu are present in the sample during the reaction.

Analysis of the residuals [Figs. 1(d) and 1(f)], in addition to verifying the existence of the intermediate phase, allows to “trap” the intermediate phase, i.e., isolate the time  $t^*$  when the intermediate phase dominates the data [ $y(t^*)=1$ , see Eq. (2)]. We associate  $t^*$  with the maximum in the residual plot when the fit was done with two principal components only. So obtained value of  $t^*$  allows us to isolate absorption coefficient  $\mu_{\text{int}}(E)$  corresponding to the intermediate phase, from the time series of all absorption data, and use them in the analysis of structure and kinetics as described below.

From the above discussion, in this process the three data sets corresponding to the starting phase,  $\mu_{\text{st}}(E)$ , intermediate phase,  $\mu_{\text{int}}(E)$ , and the end phase,  $\mu_{\text{end}}(E)$ , can all be represented by a linear combination of the three principal components obtained by PCA. By rotating these three-component vectors to the new basis formed by  $\mu_{\text{st}}(E)$ ,  $\mu_{\text{int}}(E)$ , and  $\mu_{\text{end}}(E)$ , we can now use this new triad to reproduce all data in the time series. Such reproduction can be achieved by a linear combination fit, which results in mixing fractions  $x(t)$ ,  $y(t)$ , and  $z(t)$  described earlier [Eq. (2)]. The mixing fraction as a function of time for such a three-phase reaction is illustrated in Fig. 2(a), which was obtained for the TR reduction of  $\text{Ce}_{0.8}\text{Cu}_{0.2}\text{O}_2$  by 5% hydrogen at 200 °C, measured by QEXAFS. It is important to point out that all three curves vary within the  $0 < x, y, z < 1$  range, which validates our assumptions made in isolating the intermediate phase  $\mu_{\text{int}}(E)$ . Indeed, we also obtained that, by choosing different spectra as candidates for an intermediate phase, one or more curves always fell outside of this range, signifying a serious problem with the choice of the relevant compounds for adequate representation of all the TR data.

Figure 2(b) demonstrates the same analysis done for the reoxidation reaction of  $\text{Ce}_{0.8}\text{Cu}_{0.2}\text{O}_2$  at 300 °C, when only two components were necessary to reproduce all spectra in the entire time series. This result, as well as the presence of

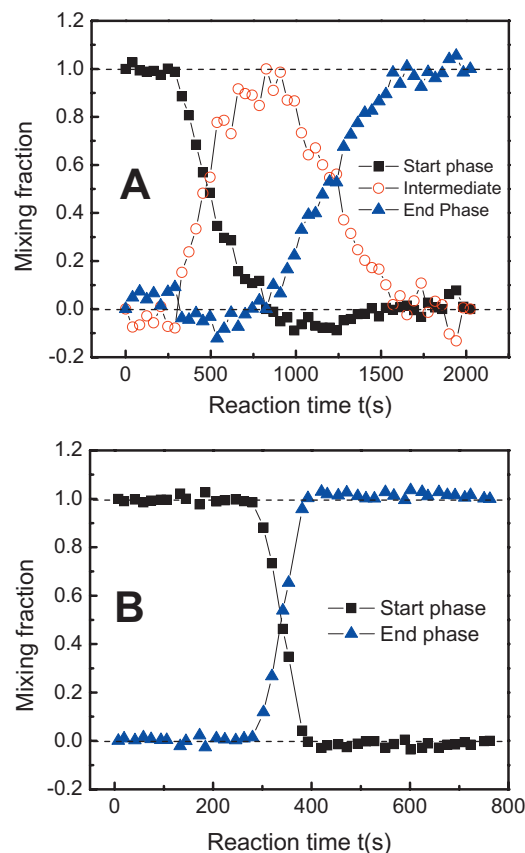


FIG. 2. (Color) TR mixing fractions of the start, the end, and the intermediate phase (when present) during the  $\text{H}_2$  reduction of Cu-doped ceria at 200 °C (a), and  $\text{O}_2$  reoxidation of Cu-doped ceria at 300 °C (b).

multiple isobestic points in the raw data, indicate independently that this process is a two-phase reaction. Thus, only  $\mu_{\text{st}}(E)$ , i.e., the reactant, and  $\mu_{\text{end}}(E)$ , the product, were applied for linear combination fit of all data in the time series in order to obtain the mixing fractions of the two phases.

We now turn our attention to the structural analysis of the intermediate phase that we identified above by PCA. The  $\mu_{\text{int}}(E)$  data in the XANES range are shown in Fig. 3(a). The spectrum has a shoulder peak ( $\sim 8980$  eV) characteristic of the  $1s$  to  $4s$  transition present in Cu (I) systems with much higher intensity than in Cu (II) ones. This peak usually is regarded as the signature feature for Cu (I) oxidation state complex.<sup>29</sup> Moreover, there are other features in the  $\mu_{\text{int}}(E)$  data, in both XANES and EXAFS ranges, resembling those in pure  $\text{Cu}_2\text{O}$ .

The  $k^2$ -weighted EXAFS data of the intermediate phase are shown in Fig. 3(a), inset. In order to analyze the local structure of the intermediate phase during reduction with hydrogen, we performed theoretical analysis of its EXAFS data using FEFF. In our analysis, we constructed model Cu–O and Cu–Cu EXAFS signals by using theoretical scattering amplitudes  $f(k)$  and phase  $\delta(k)$  of the photoelectron as generated by FEFF6 for a reference structure of  $\text{Cu}_2\text{O}$ . Due to the property of transferability of  $f(k)$  and  $\delta(k)$  between compounds that have the same central (x-ray absorbing) atom and similar atomic environment surrounding it, best fit results for the intermediate structure will not depend on the choice of the model structure. We varied the Cu–O and

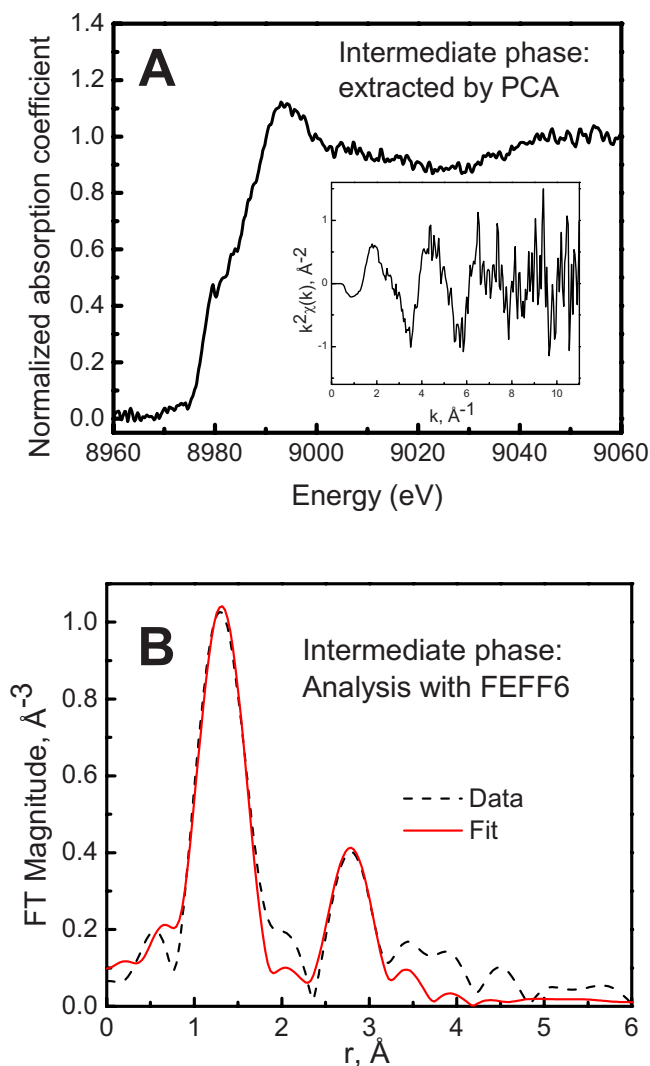


FIG. 3. (Color online) Cu  $K$ -edge XANES and  $k^2$ -weighted EXAFS (inset) data extracted by PCA for the reaction intermediate during the TR  $H_2$  reduction of Cu-doped ceria at 200 °C (a); Fourier transform magnitudes of the data (dots) and FEFF6 fit (solid) of the intermediate phase (b).

Cu–Cu bond lengths ( $R$ ) and their disorders ( $\sigma^2$ ), as well as the coordination numbers ( $N$ ) of these bonds, in the fits. The best fit is shown in Fig. 3(b) and numerical results are given in Table I. Best fit results for the coordination number ( $2.2 \pm 0.5$ ) and the bond distance ( $1.86 \pm 0.02$  Å) of Cu–O bond agree well with the  $Cu_2O$  structure (two Cu–O nearest

neighbor bonds with the bond length of 1.85 Å). However, a relatively low Cu–Cu coordination number ( $5.8 \pm 3.5$ ) compared to the bulk value of 12 and slightly expanded bond distance ( $3.07 \pm 0.02$  Å) relative to the bulk value of 3.02 Å in  $Cu_2O$  (Ref. 30) (Table I) indicate that the local structure around Cu in the intermediate phase in this reaction differs from that in bulk  $Cu_2O$ . Such difference can only be discovered by a systematic analysis described here. It is likely to be caused by the fact that copper is a dopant in ceria matrix, and it substitutes for Ce sites in the reaction starting phase (see below). This observation allows us to propose that the reduction process of copper involves interaction with the ceria matrix; which thus has a different nature, and thus a different local structure of reaction intermediate relative to the reduction reaction of pure CuO where an intermediate phase was shown by TR-EXAFS to have the same local structure as bulk  $Cu_2O$ .<sup>1,31</sup>

The analysis of local structure around Cu in the starting phase was done by FEFF fit as well. The best fit results are presented in Table I. The coordination number of the Cu–O bond is  $3.3 \pm 0.2$ , which is close but slightly smaller than the value of 4 in the ideal CuO structure. The difference from pure CuO structure was also revealed in the best fit value of the Cu–O bond length of  $1.93 \pm 0.01$  Å, which is shorter than the ideal 1.95–1.96 Å in bulk CuO. The difference in the Cu–O environment from the bulk CuO is consistent with the previous findings that no CuO or  $Cu_2O$  phases have been detected in XRD of copper-doped ceria, suggesting the dopant copper atoms are embedded in the fcc structure of ceria.<sup>31</sup> Density functional theory calculations have further proposed such a structure of copper-doped ceria, in which Cu substitutes at the Ce site and distorts to form square planar geometry of Cu with four Cu–O bonds with distances ranging from 1.92 to 1.95 Å.<sup>31</sup>

Finally, we will describe the nature of the final phase in the reaction. The  $H_2$  reduction of Cu-doped ceria resulted in metallic copper as the final product, demonstrated by the bond distances of  $2.52 \pm 0.01$  and  $3.54 \pm 0.02$  Å for two nearest neighbor Cu–Cu bonds, respectively (Table I). These distances correspond to the 2.55 and 3.61 Å values of Cu–Cu distances,<sup>30</sup> respectively, characteristic for bulk copper, albeit systematically shorter than in the bulk. One of the possibilities of such shortening is the size effect that causes compression of small metal clusters, which is shown in the

TABLE I. EXAFS results obtained by FEFF6 fitting analysis of the reaction phases during hydrogen reduction reaction of Cu/ceria system at 200 °C. Given also are relevant quantities obtained here for the following references: CuO,  $Cu_2O$ , and Cu at room temperature.

	Reaction phases			Standards		
	Starting	Intermediate	End	CuO	$Cu_2O$	Cu
$N_{Cu-O}$	$3.3 \pm 0.2$	$2.2 \pm 0.5$	$0.6 \pm 0.4$	4=2+2	2	...
$N_{Cu-Cu}$	...	$5.8 \pm 3.5$	$7.9 \pm 0.9$	10=4+4+2	12	12
$R_{Cu-O}$ (Å)	$1.93 \pm 0.01$	$1.86 \pm 0.02$	$1.85 \pm 0.03$	1.95 1.96 2.90 3.08	1.85	...
$R_{Cu-Cu}$ (Å)	...	$3.07 \pm 0.02$	$2.52 \pm 0.01$	3.17	3.02	2.55

lower coordination number of the first Cu–Cu shell ( $7.9 \pm 0.9$ ) relatively to 12 in the bulk Cu. Thus, our fitting analysis of the starting, intermediate, and end phases adds credence to the main conclusion from the PCA that the reduction process involves a spectroscopically and structurally unique intermediate phase.

#### IV. DISCUSSION

A new method of data analysis of *in situ* TR-XAFS, combining PCA with theoretical fitting of the intermediate phase, was illustrated here on the examples of reduction and reoxidation of copper/ceria system studied by QEXAFS. Not having an easy access to the intermediate phases is the most common scenario for all TR processes. Developing robust data analysis methodology is particularly timely due to the emerging new opportunities at the new synchrotron sources that will be applicable for investigation of ultrafast processes by pump-probe methods of XAS.<sup>23,32</sup> Among many types of reactions that occur very fast, several alternatives to the real time approach, such as freeze-quit,<sup>13</sup> stop-flow<sup>33</sup> methods of physical trapping and ligand-binding,<sup>34</sup> structural encapsulation,<sup>35</sup> and site-directed mutagenesis<sup>36</sup> methods of chemical trapping have been commonly used. The time resolution in these experiments is achieved by either stopping the reaction rapidly at a certain moment of time or lower the free energy for a particular intermediate.<sup>9,37</sup> However, these intermediate phases are not measured *in situ* and thus the authenticity and the very interpretation of trapped phases as *true intermediates* are questionable since the reaction pathway is modified. Our method of data analysis suits well the recently developed real time, *in situ* data collection of TR x-ray spectra.

We would like to point out that XAFS is only sensitive to the local atomic and electronic properties of nearest environment surrounding metal atoms in reacting species. This method is, therefore, limited to those reaction systems where metals play important roles (e.g., catalysts) in reactions. In some cases, like those described in this article, the relatively narrow (and thus suitable for fast timing experiments) XANES region of the x-ray absorption coefficient can be selected for PCA since XANES in many metals is very sensitive to the changes in their electronic structure and local atomic geometry during chemical transformations. However, the EXAFS range can be used instead of XANES if absorbing atom is spectroscopically silent (e.g., Zn).<sup>12,22</sup>

In summary, we proposed a new model-independent method of analyzing short-living reaction intermediates by *in situ* x-ray spectroscopy. Its strength is in the application of PCA to detect intermediate phase or phases, and the subsequent theoretical fitting of the intermediate phase isolated from the experimental data by PCA. Its implementation can be easily automated to contribute to the recently emerging efforts in developing rapid throughput data analysis methods. This method opens a new opportunity in studying real time, including recently developed ultrafast, processes by synchrotron XAS.

#### ACKNOWLEDGMENTS

We acknowledge the U.S. DOE Grant No. DE-FG02-03ER15476 (A.I.F. and Q.W.) for financial support of this work. Work at the NSLS was supported by the U.S. DOE Grant Nos. DE-FG02-03ER15688 (A.I.F.) and DE-AC02-98CH10886 (J.C.H.). The NSLS is supported by the divisions of Materials and Chemical Sciences of U.S. DOE.

- <sup>1</sup>X. Q. Wang, J. C. Hanson, A. I. Frenkel, J. Y. Kim, and J. A. Rodriguez, *J. Phys. Chem. B* **108**, 13667 (2004).
- <sup>2</sup>X. Q. Wang, J. A. Rodriguez, J. C. Hanson, D. Gamarra, A. Martinez-Arias, and M. Fernandez-Garcia, *J. Phys. Chem. B* **110**, 428 (2006).
- <sup>3</sup>D. Tibiletti, A. Amieiro-Fonseca, R. Burch, Y. Chen, J. M. Fisher, A. Gouet, C. Hardacre, P. Hu, and A. Thompsett, *J. Phys. Chem. B* **109**, 22553 (2005); X. Wang, J. A. Rodriguez, J. C. Hanson, M. Perez, and J. Evans, *J. Chem. Phys.* **123**, 221101 (2005); J. A. Rodriguez, X. Wang, P. Liu, W. Wen, J. C. Hanson, J. Hrbek, M. Perez, and J. Evans, *Top. Catal.* **44**, 73 (2007).
- <sup>4</sup>W. Wen, L. Jing, M. G. White, N. Marinkovic, J. C. Hanson, and J. A. Rodriguez, *Catal. Lett.* **113**, 1 (2007).
- <sup>5</sup>E. M. Siegbahn, *Q. Rev. Biophys.* **36**, 91 (2003); K. D. Karlin, *Science* **262**, 1499 (1993).
- <sup>6</sup>C. Berthomieu and R. Hienerwadel, *Biochim. Biophys. Acta* **1707**, 51 (2005); S. J. George, J. W. A. Allen, S. J. Ferguson, and R. N. F. Thorneley, *J. Biol. Chem.* **275**, 33231 (2000); T. Kitagawa and T. Ogura, *J. Bioenerg. Biomembr.* **30**, 71 (1998); A. Sucheta, K. E. Georgiadis, and O. Einarsson, *Biochemistry* **36**, 554 (1997).
- <sup>7</sup>W. H. Woodruff, O. Einarsson, and R. B. Dyer, *Proc. Natl. Acad. Sci. U.S.A.* **88**, 2588 (1991).
- <sup>8</sup>B. Campanini, F. Speroni, E. Salsi, P. F. Cook, S. L. Roderick, B. Huang, S. Bettati, and A. Mozzarelli, *Protein Sci.* **14**, 2115 (2005).
- <sup>9</sup>J. Hajdu, R. Neutze, T. Sjogren, K. Edman, A. Szoke, R. Wilmouth, and C. M. Wilmot, *Nat. Struct. Biol.* **7**, 1006 (2000).
- <sup>10</sup>S. Rajagopal, K. S. Kostov, and K. Moffat, *J. Struct. Biol.* **147**, 211 (2004); J. Wang and S. E. Ealick, *Acta Crystallogr., Sect. D: Biol. Crystallogr.* **60**, 1579 (2004).
- <sup>11</sup>H. Dau and M. Haumann, *J. Synchrotron Radiat.* **10**, 76 (2002).
- <sup>12</sup>J. E. Penner-Hahn, *Coord. Chem. Rev.* **249**, 161 (2005).
- <sup>13</sup>O. Kleinfeld, A. Frenkel, J. M. L. Martin, and I. Sagi, *Nat. Struct. Biol.* **10**, 98 (2003).
- <sup>14</sup>T. Ressler, O. Timpe, T. Neisius, J. Find, G. Mestl, M. Dieterle, and R. Schlogl, *J. Catal.* **191**, 75 (2000).
- <sup>15</sup>J. Helbing, L. Bonacina, R. Pietri, J. Bredenbeck, P. Hamm, F. v. Mourik, F. Chaussard, A. Gonzalez-Gonzalez, M. Chergui, C. Ramos-Alvarez, C. Ruiz, and J. López-Garriga, *Biophys. J.* **87**, 1881 (2004).
- <sup>16</sup>T. Ressler, *Anal. Bioanal. Chem.* **376**, 584 (2003).
- <sup>17</sup>A. D. McNaught and A. Wilkinson, *IUPAC Compendium of Chemical Terminology: The Gold Book*, 2nd ed. (Blackwell Science, Oxford, 1997).
- <sup>18</sup>E. R. Mallinoski, *Factor Analysis in Chemistry*, 2nd ed. (Wiley, New York, 1991).
- <sup>19</sup>S. Beauchemin, D. Hesterberg, and M. Beauchemin, *Soil Sci. Soc. Am. J.* **66**, 83 (2002); S. R. Wasserman, P. G. Allen, D. K. Shuh, J. J. Bucher, and N. M. Edelstein, *J. Synchrotron Radiat.* **6**, 284 (1999).
- <sup>20</sup>T. Ressler, J. Wong, J. Roos, and I. L. Smith, *Environ. Sci. Technol.* **34**, 950 (2000); R. Terzano, M. Spagnuolo, B. Vekemans, W. De Nolf, K. Janssens, G. Falkenberg, S. Flore, and P. Ruggiero, *ibid.* **41**, 6762 (2007).
- <sup>21</sup>A. C. Scheinost, R. Kretzschmar, S. Pfister, and D. R. Roberts, *Environ. Sci. Technol.* **36**, 5021 (2002).
- <sup>22</sup>A. I. Frenkel, O. Kleinfeld, S. R. Wasserman, and I. Sagi, *J. Chem. Phys.* **116**, 9449 (2002).
- <sup>23</sup>C. Bressler and M. Chergui, *Chem. Rev. (Washington, D.C.)* **104**, 1781 (2004).
- <sup>24</sup>J. A. Rodriguez, J. Y. Kim, J. C. Hanson, M. Perez, and A. I. Frenkel, *Catal. Lett.* **85**, 247 (2003).
- <sup>25</sup>G. Sarret, J. Balesdent, L. Bouziri, J. M. Garnier, M. A. Marcus, N. Geoffroy, F. Panfili, and A. Manceau, *Environ. Sci. Technol.* **38**, 2792 (2004).
- <sup>26</sup>I. So, D. P. Siddons, W. A. Caliebe, and S. Khalid, *Nucl. Instrum Methods Phys. Res. A* **582**, 190 (2007).
- <sup>27</sup>FORTRAN software for QEXAFS data processing was developed by the members of Synchrotron Catalysis Consortium ([www.yu.edu/scc](http://www.yu.edu/scc)) and is available upon request to [scc@yu.edu](mailto:scc@yu.edu).

- <sup>28</sup>J. Y. Kim, J. A. Rodriguez, J. C. Hanson, A. I. Frenkel, and P. L. Lee, *J. Am. Chem. Soc.* **125**, 10684 (2003); J. A. Rodriguez, J. C. Hanson, A. I. Frenkel, J. Y. Kim, and M. Perez, *ibid.* **124**, 346 (2002).
- <sup>29</sup>M. C. Hsiao, H. P. Wang, and Y. W. Yang, *Environ. Sci. Technol.* **35**, 2532 (2001); G. Sankar, P. R. Sarode, and C. N. R. Rao, *Chem. Phys.* **76**, 435 (1983); P. R. Sarode, G. Sankar, and C. N. R. Rao, *Proc.-Indian Acad. Sci., Chem. Sci.* **92**, 527 (1983).
- <sup>30</sup>R. W. G. Wyckoff, *Crystal Structures* (Interscience, New York/Wiley, New York, 1963).
- <sup>31</sup>X. Q. Wang, J. A. Rodriguez, J. C. Hanson, D. Gamarra, A. Martinez-Arias, and M. Fernandez-Garcia, *J. Phys. Chem. B* **109**, 19595 (2005).
- <sup>32</sup>M. Saes, C. Bressler, F. van Mourik, W. Gawelda, M. Kaiser, M. Chergui, C. Bressler, D. Grolimund, R. Abela, T. E. Glover, P. A. Heimann, R. W. Schoenlein, S. L. Johnson, A. M. Lindenberg, and R. W. Falcone, *Rev. Sci. Instrum.* **75**, 24 (2004).
- <sup>33</sup>K. Zhang, R. F. Liu, T. Irving, and D. S. Auld, *J. Synchrotron Radiat.* **11**, 204 (2004).
- <sup>34</sup>I. Schlichting and K. Chu, *Curr. Opin. Struct. Biol.* **10**, 744 (2000).
- <sup>35</sup>V. M. Dong, D. Fiedler, B. Carl, R. G. Bergman, and K. N. Raymond, *J. Am. Chem. Soc.* **128**, 14464 (2006).
- <sup>36</sup>J. M. Bolduc, *Science* **270**, 365 (1995).
- <sup>37</sup>B. L. Stoddard, *Nat. Struct. Biol.* **3**, 907 (1996); B. L. Stoddard, *Methods* **24**, 125 (2001); K. Moffat, *Chem. Rev. (Washington, D.C.)* **101**, 1569 (2001).